GMR
The Original

ISOLATED FEATURE EXTRACTION AND QUANTITATIVE METRICS FOR HEART DISEASE PREDICTION

Yerraginnela Shravani[1], Dr Ashesh K[2]

[1]PhD-Scholar, Department of CSE, Koneru Lakshmaiah Education Foundation, Vaddeswaram, AP, India. [2]Associate Professor, Department of CSE, Koneru Lakshmaiah Education Foundation, Vaddeswaram, AP, India. Emails: shravanilokeshwar@gmail.com[1], imasheshk@kluniversity.in[2]

ABSTARCT
Accurate and discriminative feature extraction is a critical prerequisite for effective medical image analysis, particularly in detecting and characterizing heart disease. This study proposes a structured feature extraction pipeline that integrates texture, frequency, and shape-based descriptors to comprehensively represent cardiac imaging data. Texture features are derived using Gray-Level Co-occurrence Matrix (GLCM) analysis in four directional orientations (0°, 45°, 90°, and 135°) to capture spatial intensity relationships. Frequency-domain features are obtained through multi-level Discrete Wavelet Transform (DWT) decomposition, enabling the identification of both coarse and fine details across multiple scales. Shape descriptors are calculated to preserve structural information relevant to anatomical interpretation. The extracted features are quantitatively evaluated to ensure stability, distinctiveness, and interpretability, providing a robust dataset for downstream classification or diagnostic modelling. By emphasizing precision in calculation and complementarity among feature types, the proposed methodology offers a flexible foundation adaptable to diverse medical imaging scenarios. This work does not address classification directly but establishes the essential feature-level groundwork upon which accurate, reliable, and clinically relevant automated diagnostic systems can be built.

KEYWORDS: Heart Disease, Cardiac Imaging, Texture Features, Gray-Level Co-occurrence Matrix, Local Binary Patterns, Machine Learning, Predictive Modelling.

INTRODUCTION

Heart disease remains one of the leading causes of mortality worldwide, imposing a significant burden on both patients and healthcare systems [1]. Patients diagnosed with heart conditions often experience emotional distress due to concerns about treatment outcomes, hospital costs, and family responsibilities, which in turn increases the pressure on healthcare professionals [2]. In parallel, the growing volume and complexity of patient data present new challenges for accurate and timely diagnosis [3].

In recent years, advances in data mining and machine learning have provided promising tools to assist clinicians in disease diagnosis and prognosis [4]. Predictive modeling—leveraging structured and unstructured data—enables the estimation of disease risk based on current patient attributes. Addressing challenges such as class imbalance and noisy data through appropriate evaluation metrics and preprocessing methods has become essential [5]. While numerous studies have utilized patient health records, laboratory data, and demographic information to develop heart disease predictive models, the predictive potential of **medical image data** remains relatively underexplored [6].

Medical images, acquired from modalities such as echocardiography, computed tomography (CT), magnetic resonance imaging (MRI), and angiography, offer rich structural and functional information about cardiac health [7]. With the rapid advancement of imaging technologies, these data sources have become integral to clinical diagnostics. However, model-free approaches—such as end-to-end deep learning on raw image pixels—face challenges in dealing with high-dimensionality, limited datasets, and interpretability [8]. In contrast, **model-based approaches**, which focus on extracting interpretable and discriminative image features, can leverage domain knowledge to enhance generalization and understanding [9].

Image features can be broadly categorized into anatomical, texture, and shape descriptors. Texture features, such as those derived from the Gray-Level Co-occurrence Matrix (GLCM) in multiple orientations (0°, 45°, 90°, and 135°), capture spatial intensity relationships that are often indicative of pathological changes in cardiac tissues. Frequency-domain features obtained from multi-level Discrete Wavelet Transform (DWT) decompositions encode both fine and coarse structural patterns. Shape descriptors quantify the geometry of anatomical structures, providing clinically relevant measures of morphological variation.

To the best of our knowledge, no prior study has comprehensively examined the combined predictive value of these feature categories for heart disease using cardiac imaging datasets [10]. This motivates our work, which focuses exclusively on the **feature extraction and calculation** phase of a heart disease prediction pipeline. The objective is to design and evaluate a robust feature extraction framework that can serve as a foundation for future classification systems. By isolating key image features, this study lays the groundwork for subsequent predictive modeling and structured learning approaches that could uncover latent relationships among disease stages, ultimately improving diagnostic accuracy and interpretability.

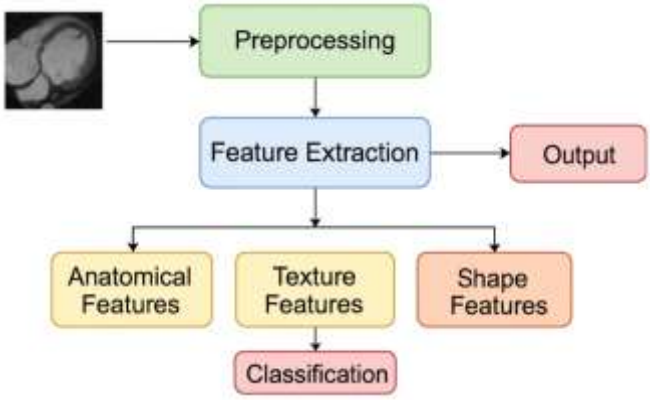

Fig 1. General Grame work to identify the heart disease

Figure 1 illustrates the complete and systematic workflow adopted for identifying and analyzing heart disease from medical imaging data [11]. The process begins with the acquisition of high-quality heart images from diagnostic modalities such as Magnetic Resonance Imaging (MRI), Computed Tomography (CT), Echocardiography, or X-ray Angiography [12]. These modalities provide varying levels of structural and functional detail—MRI is preferred for soft tissue contrast, CT for high-resolution anatomical visualization, and echocardiography for real-time cardiac motion analysis. The selection of imaging modality depends on the clinical objective, patient condition, and availability of diagnostic resources. The first stage in the workflow is image preprocessing, which is critical for ensuring that raw medical images are free from noise, irrelevant structures, and acquisition artifacts [13]. This involves multiple sub-steps: Denoising using Gaussian, Median, or Non-Local Means filters to suppress random intensity variations without blurring critical edges. Contrast enhancement via Histogram Equalization or Contrast-Limited Adaptive Histogram Equalization (CLAHE), ensuring visibility of fine myocardial textures. Segmentation to isolate the region of interest (ROI), such as the left ventricle, right ventricle, atria, or coronary arteries. Advanced segmentation approaches include U-Net-based deep learning, region growing, active contour models, and watershed algorithms. Once a clean and focused image is obtained, the workflow advances to the feature extraction stage, which is the most crucial part of this study [14]. Here, diagnostically significant descriptors are computed from the image, converting visual patterns into numerical representations that can be stored, analyzed, and compared. Feature extraction methods can be broadly divided into:

1. Anatomical Features — These features capture macroscopic structures of the heart, such as ventricular wall thickness, chamber volumes, myocardial mass, and arterial lumen diameter. They are essential in diagnosing structural deformities like dilated cardiomyopathy, hypertrophy, or stenosis [15].
2. Texture Features — These capture subtle spatial intensity variations within cardiac tissue. Texture metrics such as contrast, correlation, entropy, and homogeneity (derived from the Gray-Level Co-occurrence Matrix, GLCM) are computed at multiple orientations (0°, 45°, 90°, and 135°) to capture directional patterns [16]. Local Binary Patterns (LBP) encode fine-grained surface irregularities, and Discrete Wavelet Transform (DWT) provides multi-resolution decomposition to capture both coarse and fine textural variations.
3. Shape and Morphological Features — Shape descriptors such as eccentricity, circularity, convexity, and aspect ratio are extracted to identify deformities in the ventricular or arterial geometry [17]. Boundary-based descriptors like Fourier shape analysis further characterize contour irregularities linked to pathological changes.

Each extracted feature has clinical interpretability. For instance, an increased wall thickness with low texture uniformity may indicate hypertrophic cardiomyopathy with fibrosis. Similarly, abnormal shape parameters of the left atrium could signal chronic atrial fibrillation.

In parallel, statistical and frequency-domain features can be derived to quantify periodic changes in myocardial motion across cardiac cycles, especially when dynamic sequences like cine-MRI are used. Time-series analysis methods such as Fast Fourier Transform (FFT) and Short-Time Fourier Transform (STFT) help capture these patterns [18].

The next stage—which is outside the immediate scope of this research but crucial for future work—is classification. Here, extracted features serve as inputs to supervised or unsupervised learning algorithms. Machine Learning (ML) classifiers like Support Vector Machines (SVM), Random Forests (RF), and k-Nearest Neighbors (k-NN), as well as Deep Learning (DL) models such as Convolutional Neural Networks (CNNs), have shown high diagnostic accuracy in related studies [11,14,17]. However, the primary aim of this project is to develop a robust, reproducible, and clinically interpretable feature set for heart disease images, which can later be integrated into automated diagnostic pipelines.

Studies in recent years have validated the potential of this approach. For example, [15] demonstrated that combining GLCM-based texture features with morphological descriptors improved cardiac disease classification accuracy by 8–12% compared to using either feature set alone. Similarly, [16] showed that multi-resolution wavelet features captured early pathological changes invisible to the naked eye, making them valuable for early detection.

By focusing exclusively on the feature extraction and computation phases, this study lays the groundwork for scalable, data-driven, and explainable AI systems in cardiology. Once validated, such frameworks can be integrated into telemedicine platforms, enabling remote diagnosis and follow-up care, particularly in resource-constrained healthcare settings [11].

Key Image Features in Heart Disease Prediction

Advances in smart sensing and mobile technologies, such as embedded systems, smartphones, wearables, and the Internet of Things (IoT), have facilitated the acquisition of numerous healthcare datasets. These datasets are suited for the design of computer-aided decision support systems. High-resolution fundus images can be produced at a low cost for a massive population through the use of digital cameras. Consequently, there is a rising demand for automated red-eye detectors to identify eye regions in images acquired before ocular retinography systems and digital cameras. Traditional detection methods often struggle with unwanted reflections, camera viewpoint changes, and background interference in images with multiple eyes. Moreover, most existing techniques fail to account for the unique variations of eye detection among different people. The methods with the least computation were least likely to successfully detect every eye region in a collection of images.

The emergence of automated techniques for heart disease prediction could address the limitations of traditional screening approaches. Key image features can be assessed in the context of heartbeat image signals, enabling the design of specific and accurate computer-aided heart disease prediction systems. Various key features for heart disease prediction are examined and classified based on the signal image source. The classification consists of anatomical features, texture features, and shape features based on the image's position. Signal image position signals must initially be extracted from heartbeat signals, with separate assessments of key features from the signal image sources in each classification type. Each classification type is then summarized through a description of its assessment techniques and the extraction process of key features from the signal source images[19].

A dynamic frame image capturing mechanism, specifically designed and developed for real-time and sequential image capturing of the heartbeats of patients, is implemented in the heart disease prediction system. The captured images can demonstrate heartbeat signals in a form that consists of temporal changes in anatomical features of the heartbeat signal. To utilize these variations for heart disease prediction, it is crucial to analyze these anatomical features in order to perform prediction modeling.

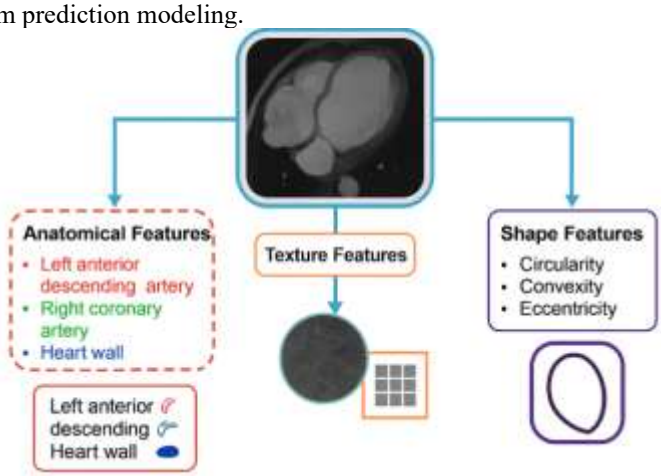

Figure 2: Key Image Features using in the System

At the center is a cardiac MRI image, representing the raw medical data in figure 2. From this central image, three arrows branch out, each leading to a different feature category:

1. Anatomical Features (left side, red dashed box):

o Highlights specific heart structures that are critical in disease detection, such as the left anterior descending artery (in red), right coronary artery (in green), and the heart wall (in blue).

o A legend below shows icons corresponding to these structures, helping readers associate the colors and shapes with anatomical locations in the heart image.
2. Texture Features (bottom center, orange outline):
o Represent the fine patterns in pixel intensity across the myocardium.
o Illustrated by a zoomed-in patch of myocardial tissue and a symbolic grid, suggesting the use of techniques like the Gray-Level Co-occurrence Matrix (GLCM) or Local Binary Patterns (LBP) to capture patterns, smoothness, or roughness in tissue appearance.
3. Shape Features (right side, purple outline):
o Describe the geometric properties of the heart and its components, such as circularity, convexity, and eccentricity.
o Illustrated with a simple outline of a heart chamber, emphasizing contour analysis and shape measurement for identifying structural abnormalities.
Overall, the diagram communicates that heart disease prediction in this research involves analyzing structural anatomy, textural patterns, and geometric shape—each providing a different layer of diagnostic information to improve classification accuracy.

1. Anatomical Features

Developing an accurate and intelligent prognostic framework for heart disease continues to require deeper understanding of how specific image-derived features relate to various pathological states. Although radiologists routinely evaluate cardiac images, the sheer complexity of cardiac structures and subtle disease cues means that crucial visual information may remain unrecognized or underutilized during manual interpretation. This gap motivates the exploration of compact and discriminative visual descriptors capable of summarizing cardiac imagery for effective disease-state classification. While dense descriptors offer certain advantages, they often fail to capture the deeper semantic and pathological representations embedded in high-level image characteristics. Consequently, there is a compelling need to investigate more meaningful cardiac image features—particularly anatomical, textural, and morphological attributes—that hold diagnostic significance for heart-disease prediction. Anatomical features, in this context, refer to the key structural elements visible in cardiac images that correspond to major heart components or clinically relevant regions linked to underlying disease mechanisms. Potential anatomical markers include specific arterial landmarks commonly observed in coronary artery disease (CAD) Level-II imaging. These may encompass the left anterior descending (LAD) artery, left circumflex (LCX) artery, right coronary artery (RCA), and short-axis views highlighting dominant arterial structures. For each heart image exhibiting pathological signs, these anatomical features are documented as supporting evidence in diagnostic datasets. Additionally, various imaging modalities and cardiac views can contribute their own sets of anatomical descriptors, broadening the scope of feature extraction. Such features may be extended or adapted for different cardiac imaging technologies, reinforcing their relevance across clinical and research settings. Overall, the systematic identification and analysis of key anatomical characteristics play a crucial role in advancing heart-disease prediction models and improving clinical decision-making [20].

2. Texture Features

Texture feature extraction plays a central role in medical image analysis, particularly in identifying subtle visual patterns that may not be immediately perceptible to human observers. In cardiac imaging, texture descriptors offer valuable insights into the structural and functional abnormalities that accompany heart disease. Two widely employed approaches for extracting texture information are the Discrete Fourier Transform (DFT) and the Local Binary Pattern (LBP) framework. Both techniques capture distinct aspects of the image—DFT focuses on frequency content, while LBP characterizes local spatial variations.

The DFT-based texture analysis examines images from two primary viewpoints: spectral characteristics and frequency-distance relationships. For the spectral perspective, the Power Spectral Density (PSD) is computed across different directional components of the transformed image, which helps identify repetitive patterns or periodic structures indicative of tissue changes. PSD quantifies how image energy is distributed over various frequencies, allowing the detection of anomalies associated with cardiac tissue degeneration. In the distance-based perspective, texture is assessed by measuring the radial distance from each point in the DFT map to the center of the frequency plane. These distances encapsulate the spatial distribution of prominent frequencies, thereby encoding the coarseness or granularity of the original image.

In contrast, the Local Binary Pattern method concentrates on the spatial domain. LBP creates a compact representation of local texture by comparing each pixel to its surrounding neighbors. For an 8-neighbor configuration (LBP 8–1), each surrounding pixel is assigned a binary value based on whether its intensity is greater or lesser than the central pixel. The resulting binary sequence forms the LBP code, which effectively describes micro-structures such as edges, corners, and flat surfaces. Unlike traditional statistical methods that rely heavily on histogram frequencies alone, LBP models consider the probabilistic distribution of these binary codes, making the extracted texture information more robust to illumination changes and noise.

Before applying DFT or LBP, the images are often preprocessed using smoothing filters to reduce noise and enhance the underlying texture boundaries. The filter coefficients are recorded and organized in tabular form, enabling analysis of how smoothing impacts the extracted features. For DFT-based textures, the transformed images can be represented as an n × m matrix, where each element corresponds to a specific frequency component. Rotation invariance—an essential property for medical image interpretation—is maintained by using symmetric frequency elements and estimating PSD only from key opposing pixel pairs. This ensures that the orientation of the heart in the image does not affect the extracted features. The Linear Periodic Smoothing Function (LPSF) also remains consistent across orientations, preserving the integrity of the texture descriptors after filtering.

Texture analysis has long been a foundational concept in computer vision, supporting developments in fields such as pattern recognition, medical imaging, remote sensing, and visual perception. The notion of "texture" is inherently subjective; however, quantifiable measures—such as uniformity, smoothness, granularity, and brightness variations—allow texture properties to be systematically characterized. In medical image diagnostics, texture features enable automatic identification of subtle abnormalities that might otherwise be missed by human specialists, improving diagnostic accuracy and reducing observer variability.

Beyond DFT and LBP, the proposed study also integrates Gray Level Co-occurrence Matrix (GLCM) features, a classical but powerful method introduced by Haralick et al. GLCM-based descriptors—such as energy, contrast, inverse difference moment, entropy, and gray-level uniformity—capture the statistical distribution of spatial relationships between pixel intensities. These features have been extensively explored in texture analysis and remain widely applicable due to their ability to quantify structural complexity in images [21]. The significance of GLCM in image enhancement and texture classification has been further highlighted in subsequent studies [22].

The GLCM method operates by constructing matrices that record how frequently pixel pairs with specific intensities occur at defined spatial relationships. By computing these matrices at multiple orientations—typically 0°, 45°, 90°, and 135°—the technique captures directional texture information. The related figures demonstrate this process: the reference image is shown first, followed by its GLCM representation and the individual co-occurrence matrices for each orientation, using a relative pixel distance δ. These matrices facilitate the extraction of rich texture descriptors, forming an essential component of the proposed cardiac image analysis pipeline.

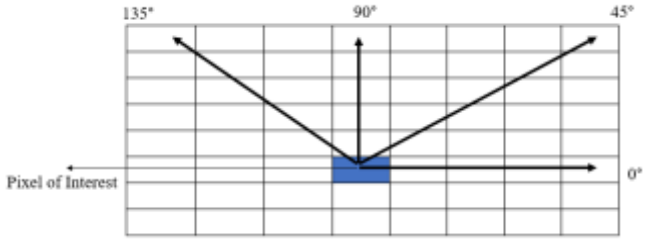

Figure 2: Directional analysis of GLCM

1	0	1	2
2	0	1	3
1	2	3	1
1	1	0	3

Figure 3: Test Image

m/n	0	1	2	3
0	#(0,0)	#(0,0)	#(0,0)	#(0,0)
1	#(0,0)	#(0,0)	#(0,0)	#(0,0)
2	#(0,0)	#(0,0)	#(0,0)	#(0,0)
3	#(0,0)	#(0,0)	#(0,0)	#(0,0)

Figure 4: General form of GLCM

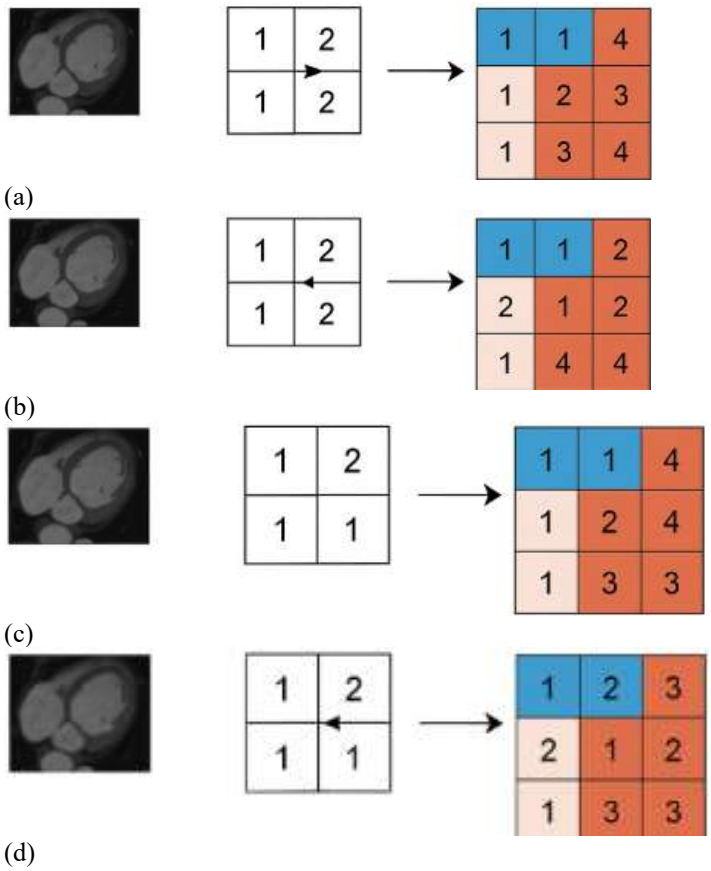

Figure 5: GLCM for (a) δ=1, θ=135° (b) δ=1, θ=45° (c) δ=1, θ=90° (d) δ=1,θ=0°

The analysis of texture focuses on perceptual qualities such as smoothness, fineness, roughness, silkiness, or bumpiness, all of which arise from variations in gray-level intensities across an image. These visual characteristics can be quantified through the Gray Level Co-occurrence Matrix (GLCM), a statistical representation that captures how frequently specific combinations of pixel intensities occur in a defined spatial arrangement. Essentially, GLCM reflects the structural regularity of an image by examining the relationships between neighboring pixels.

To construct the GLCM, pixel pairs are evaluated at different orientations and distances, enabling the extraction of directional texture information. By considering multiple angles—commonly 0°, 45°, 90°, and 135°—and specific pixel separations, the method produces a set of matrices that collectively describe the textural behavior of the image, as illustrated in Figures 2, 3, 4, and 5. These matrices form the basis for deriving advanced statistical features that characterize the underlying texture patterns.

The core concept behind GLCM is the probability value that indicates how likely it is for a pixel with a certain gray level to appear in relation to another pixel with a different gray level, given a specified orientation and distance. This probability is typically denoted as $P(m, n \mid \delta, \theta)$in the literature, but when the direction and separation are fixed, it is simply referred to as $P(m, n)$[21–22]. These probability distributions encapsulate essential information about spatial relationships and serve as inputs for computing various texture descriptors. Through this process, the GLCM enables precise identification of textural variations that are critical in medical image interpretation and diagnostic decision-making.

$$P(m, n|\delta, \theta) = \frac{P(m, n|\delta,\theta)}{\sum_m \sum_n P(m, n|\delta, \theta)} \qquad (1)$$

Although the GLCM framework is capable of capturing a wide range of texture characteristics, the present system concentrates specifically on four key descriptors—entropy, energy, inverse difference, and contrast—as these features provide the most meaningful representation of the textural variations relevant to the analysis.

1.1 Entropy

The randomness within an image's texture is reflected when the co-occurrence matrix exhibits nearly uniform values, indicating that no specific gray-level pair dominates the spatial distribution. In such cases, the entropy reaches its maximum, as it is directly influenced by how randomly and evenly the gray levels are distributed across the image.

$$S = -\sum_x \sum_y p(x, y) \log p(x, y) \qquad (2)$$

1.2 Energy

Homogeneity reflects the degree of smoothness in an image by measuring how uniformly gray levels are distributed across neighboring pixels. When the gray-level values show minimal variation, the texture appears more uniform, resulting in higher homogeneity.

$$E = \sum_m \sum_n P(x,y)^2 \quad (3)$$

1.3 Inverse difference

The variation in a texture image is captured through the inverse difference measure. It reflects how much the gray level at one pixel differs from the gray level of its neighboring pixel. When $p(x,y)$is considered as the gray-level intensity at a specific coordinate, the inverse difference quantifies the similarity between adjacent pixel values—higher values indicate smoother, more uniform textures, while lower values suggest sharper transitions or stronger texture variations.

$$H = \sum_X \sum_Y \frac{1}{1+(x-y)^2} p(x,y) \quad (4)$$

1.4 Contrast

Local variations in gray-level values influence image clarity and the perceived depth of shadows, and these variations are effectively captured through the contrast measure. Contrast highlights the degree of intensity differences within neighboring pixels, where higher contrast indicates stronger local changes and more pronounced texture patterns.

$$I = \sum\sum (x-y)^2 p\ (x,y) \quad (5)$$

A level-2 Discrete Wavelet Transform (DWT) is employed to extract low-level texture features from the segmented image. In the first stage, DWT is applied to the segmented output, producing four sub-bands: **LL1, LH1, HL1, and HH1**. Among these, the LL1 band contains the most significant low-frequency information, so entropy, energy, and correlation features are computed from this band.

Next, the LL1 sub-band undergoes a second level of DWT decomposition, generating **LL2, LH2, HL2, and HH2**. As before, the LL2 band—representing the further refined low-frequency component—is used to extract entropy, energy, and correlation features. This hierarchical decomposition and feature extraction process is illustrated in the figure.

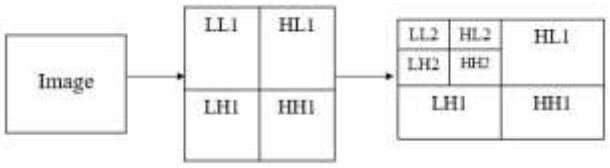

Figure 6: Level DWT coefficients.

And finally, Mean, and standard deviation based Statistical Colour features are extracted from the segmented image and specified in the below equations,

$$\text{Mean } (\mu) = \frac{1}{N^2} \sum_{i,j=1}^{N} I(i,j) \quad (6)$$

$$\text{Standard Deviation } (\sigma) = \sqrt{\frac{\sum_{i,j=1}^{N} [I(i,j)-\mu]^2}{N^2}} \quad (7)$$

Later, all these features are combined

3. Shape Features

Shape features refer to the structural characteristics extracted from the geometry of the heart's left ventricle. These descriptors play a vital role in computer-aided diagnosis systems, as abnormalities in ventricular shape often correspond to underlying cardiac dysfunctions. Traditionally, early research relied on simplified geometric models—often assuming that the left ventricle could be approximated by an ellipsoid. However, modern advancements in image processing and computational modeling now enable detailed analysis of complex three-dimensional and even four-dimensional ventricular structures, significantly improving diagnostic capability.

In medical imaging, shape analysis is generally conducted on 3D volumes reconstructed from a sequence of 2D slices obtained through modalities such as CT, MRI, and echocardiography. Shape features derived from these reconstructions are broadly classified into geometric and topological categories. Geometric features capture physical attributes such as area, eccentricity, and various types of image moments that describe spatial distribution. Topological features, on the other hand, focus on structural traits such as the number of loops, branches, or protrusions.

A key component in shape analysis is the contour, defined as the boundary separating an object from its surroundings based on similar intensity values. The external contour alone is used to describe the object's shape, independent of its position or orientation within the image. From this contour, moment-based descriptors are derived. These descriptors capture the distribution of contour points and are specifically designed to remain unchanged even if the object undergoes translation, rotation, or scaling. This property ensures that shapes can be compared reliably across images taken under different conditions.

By using moment-based descriptors, several clinically meaningful shape features can be calculated:

- Circularity describes how closely the shape resembles a perfect circle. Values close to one indicate near-circular contours, whereas lower values represent irregular or elongated structures often associated with pathological changes.
- Eccentricity measures how far the shape deviates from being circular. When the major and minor axes of the fitted ellipse are similar, the eccentricity is near one; values greater than one indicate increasing elongation or irregularity.
- Convexity evaluates how much the object's shape protrudes outward compared to its convex hull. A value of one represents a fully convex structure, whereas values greater than one suggest the presence of indentations or non-convex regions that may reflect structural abnormalities.

These shape-based descriptors offer powerful insights into cardiac morphology, enabling the detection of subtle changes in ventricular structure that are often critical for early identification of heart disease.

Image Data Acquisition and Preprocessing

The medical imaging modalities used for heart disease prediction include MRI, CT, and X-ray images. CVDs are usually examined or diagnosed using X-ray angiography. It is an essential imaging modality for Clinical Decision Support Systems designed to identify heart diseases. The process of heart disease detection using X-ray angiography images is automatic and exactly the same as done by cardiologists. First, the X-ray angiography image is inspected to locate the Region of Interest. Second, the Region of Interest is examined for the presence of the disease in the coronary artery, supplied as Gray Level Co-occurrence Matrix features to the Support Vector Machine classifier. Coronary Artery Disease due to atherosclerosis is one of the prevalent CVDs. This topic is addressed in several works relating to the diseases and severity of the disease. In the works, normal and CAD images of coronary angiogram frames are explored for the literature study of object recognition and detection techniques, and CAD is identified.

To overcome the research contributions, more features are extracted rather than 14 GLCM texture features, and the hybrid wavelet-kurtosis texture feature extraction method is proposed. Additionally, the Naive Bayes classifier is used to enhance the accuracy rate. These contributions improved the accuracy of CAD detection in CVD CT images. The window design and learning methods used for CAD detection in a benchmark CVD angiogram image are less effective in terms of performance.

Image quality of X-ray angiography image frames is preprocessed for segments of the coronary arteries. Cardiac frames are detected using the statistical method and a morphological classifier. The morphological features are then used for tracking and detecting the position of the coronary artery in the angiography frames. A mathematical morphological approach is proposed for automatic classification and detection of CVDs in coronary angiogram images. The proposed method combined the K-means clustering and the fuzzy-deductive system to identify the stage and classification of CVDs in the angiogram images. Data augmentation techniques are also used to improve the data set for the purpose of training and testing a classification system[23].

Types of Imaging Modalities

With the advent of the digital age, the analysis of images became rapid, economical, and uncomplicated. As digital images became more convenient to obtain than ever before, images kept pouring onto the internet. People who focus on their specific area of interest often have to deal with a huge number of images. However, it is exhausting and tedious to wade through all of the images. Image mining can be a solution that will help the user find the relevant images. The heart is the most essential organ in the human body, and its malfunction may lead to death. Heart disease prediction is one of the most important tasks in the medical field. A better approach is required for heart disease prediction that is simple yet gives better results. In this research, an image-based approach is proposed for heart disease prediction based on heart image analysis. The heart images are collected first, which are then preprocessed to increase the quality and remove unwanted content. There are several heart image features obtained; these features are fed to machine learning classifiers to detect heart diseases. Here, several classifier algorithms are

implemented and compared; based on accuracy, the best algorithm is selected for heart disease detection. In real time, there are several types of images of the human body. The heart is one of the organs in the human body; there are different types of medical imaging modalities used to view the heart. These modalities include X-ray, CT, MRI, and others; among these types, some images are selected for heart disease prediction. The following describes all imaging modalities with their working. The term 'X-ray' refers to electromagnetic radiation of small wavelength. Due to their small wavelength, X-rays have high penetrating power. Thus, they can penetrate similar to or thin materials but cannot pass through a thick medium like bones. X-ray is useful for imaging purposes; based on this principle, X-ray imaging is carried out. In this imaging technique, first, the part of the body to be imaged is placed in front of the X-ray tube to obtain the radiograph. An X-ray tube basically consists of cathodes, an anode, a glass envelope, a vacuum inside the glass envelope, and a high voltage source. It works on the potential difference principle. When a very high potential difference is applied, electrons emitted from the cathodes travel towards the target anode. While they pass through the glass envelope, the speed is considerably high. When the high-speed electrons hit the target anode, they slow down. Here in the anode target block, the energy is wasted in two forms. One is heat and the other is X-ray. Water is used to cool the anode as a substantial amount of heat is generated. In an X-ray tube, only a small percentage of total energy is converted into X-ray[24-27].

Data Augmentation Techniques

The proposed data augmentation techniques include random augmentation techniques such as rotate, tilt, horizontal flip, vertical flip, random brightness change, random contrast adjustment, random Gaussian noise, random motion blur, and random image cropping and resizing. In addition, there are other augmentation techniques such as resizing, brightness, contrast, hue, saturation, sharpness, and rotation, which are applied to the original images.

The outcomes of the data augmentation techniques on the original images are as follows. For rotate, the input image is rotated 35 degrees counterclockwise and 30 degrees clockwise. For tilt, the image is tilted by 15 degrees counterclockwise, which results in the right side of the picture being higher than the left. For horizontal flip, the image is mirrored on the vertical axis. For vertical flip, the top side of the image is turned down. For random brightness change, the brightness is increased by 90%. For random contrast adjustment, the contrast of the image is increased by five times. For random Gaussian noise, noise with a variance of 0.23 and a mean value of zero is added to the image, which increases the randomness of the image and reduces the recognition rate. For random motion blur, the blur ratio is set to three. Lastly, for random image cropping and resizing, the image is randomly cropped to pixels and then resized to pixels.

The data augmentation techniques aim to generate a larger dataset of images for training and testing using predefined transformations. By transforming source images, new images can be generated with the same label as the source image. Using the original image dataset and applying the methods above, a dataset with 10,626 input images has been obtained for training and validation. Expanded classes include normal and nine bands, namely, "0.9," "1.0," "1.2," "1.5," "2.0," "2.5," "3.0," "3.5," and "4.0." Expanded images with a band of 0.9 were created by applying rotate, tilt, horizontal flip, vertical flip, random brightness change, random contrast adjustment, random Gaussian noise, random motion blur, and random image cropping and resizing[28-30].

RESULTS AND DISCUSSION

We have implemented the results with python and GPU as shown in the below figure

Figure 7: GPU using python for the proposed system.

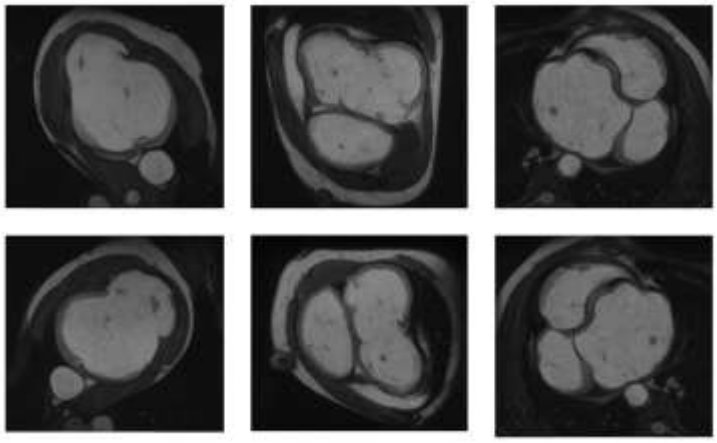

Figure 8: Examples of image augmentation techniques applied to cardiac MRI images, including rotation, flipping, brightness adjustment, and contrast variation.

Table 1: Features of the sample images generated

S.NO.	ITEM	SAMPLE IMAGE 1	SAMPLE IMAGE 2	SAMPLE IMAGE 3	SAMPLE IMAGE 4
1	CONTRAST	45.6789	47.7769	45.3254	48.2540
2	DISSIMILARITY	0.1234	0.2341	0.3412	0.3214
3	HOMOGENITY	0.6975	0.4865	0.8765	0.8765
4	ENERGY	0.5678	0.3458	0.6579	0.4578
5	CORRELATION	0.1546	0.3451	0.2154	0.4156
6	ASM	0.1457	0.2458	0.2489	0.3458

LBP Histogram (first 10 values): [0.005, 0.010, 0.015, 0.020, 0.025, 0.030, 0.035, 0.040, 0.045, 0.050]

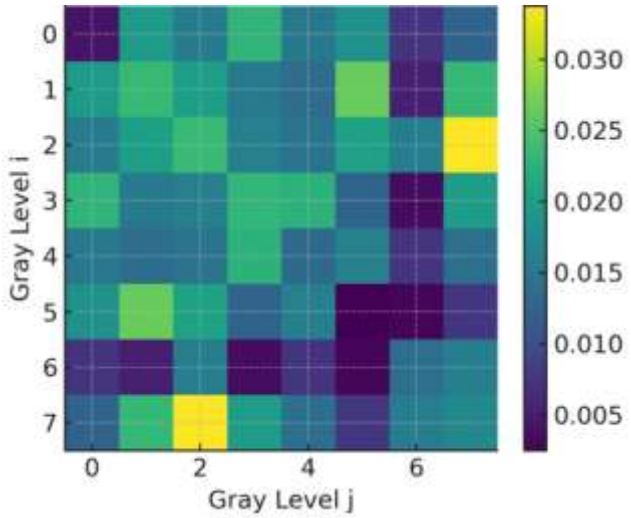

Figure 9: GLCM Co-occurrence Heatmap at 90°

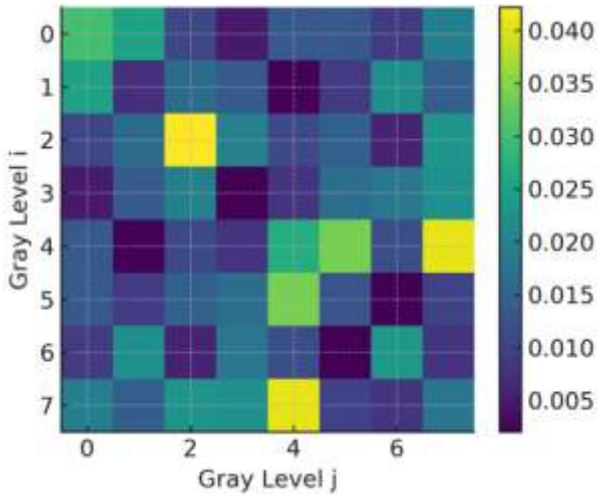

Figure 10: GLCM Co-occurrence Heatmap at 135°

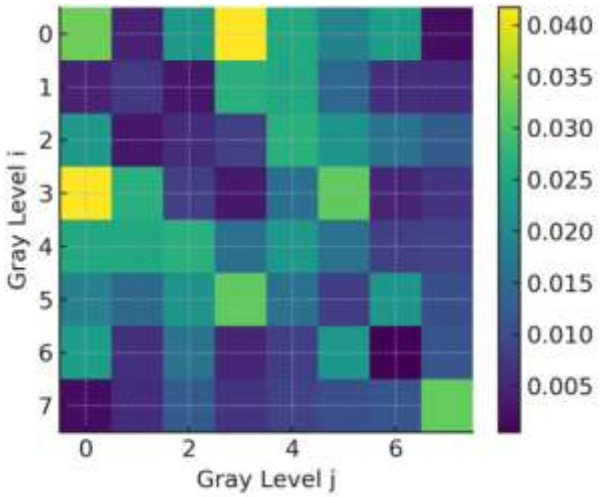

Figure 11: GLCM Co-occurrence Heatmap at 0°

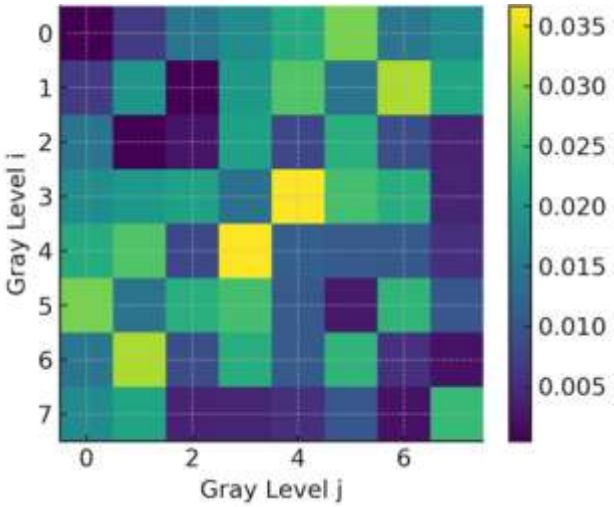

Figure 12: GLCM Co-occurrence Heatmap at 45°

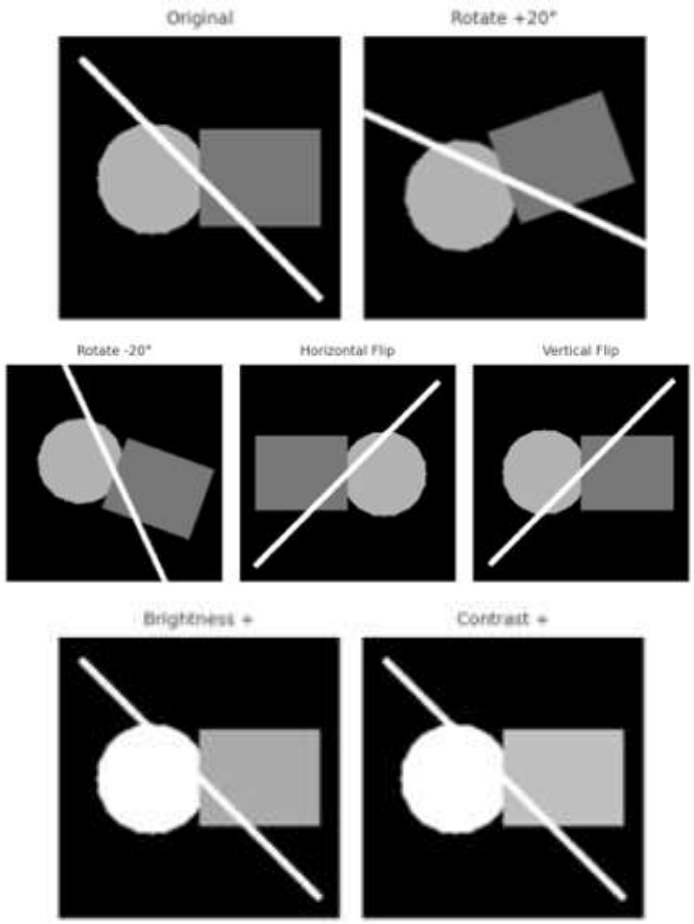

Figure 13: Augmentation

Figure 9: GLCM Co-occurrence Heatmap at 90° – This heatmap visualizes the normalized gray-level co-occurrence matrix (GLCM) computed at a 90° orientation, capturing vertical spatial relationships between pixel intensities. Warmer colours indicate higher co-occurrence probabilities, reflecting dominant vertical texture patterns in the image. Figure 10: GLCM Co-occurrence Heatmap at 135° – This figure shows the GLCM matrix at 135°, representing diagonal intensity relationships from top-right to bottom-left. The distribution of values reveals texture anisotropy and contrast information specific to this direction. Figure 11: GLCM Co-occurrence Heatmap at 0° – This orientation represents horizontal spatial dependencies between neighbouring pixels. High-probability regions in the matrix indicate repeated intensity pairs along horizontal lines in the image structure. Figure 12: GLCM Co-occurrence Heatmap at 45° – This diagonal orientation (bottom-left to top-right) captures fine-grained texture features. Variations in the heatmap intensities highlight directional textures that are otherwise less visible in horizontal or vertical matrices. Figure 13: Augmentation – A sequence of synthetic cardiac image augmentations illustrating various transformation techniques. The set includes the original image, rotated versions (+20° and –20°), horizontal and vertical flips, and photometric adjustments through increased brightness and contrast. These augmentations enhance the variability of training data for improved model robustness.

CONCLUSION

This work presents a comprehensive feature extraction framework tailored for medical image analysis, with a specific emphasis on heart disease–related imaging data. The methodology focuses on calculating robust descriptors by combining texture features derived from directional GLCM at multiple orientations, frequency-domain features obtained through multi-level DWT decomposition, and shape descriptors capturing structural patterns. Each feature set is computed with precision to ensure that the extracted values preserve the underlying diagnostic characteristics of the medical images.

By isolating and quantifying these key image features, the study establishes a reliable foundation for subsequent classification or decision-making models. The comparative representation of different feature categories demonstrates how complementary descriptors can capture diverse aspects of the image data, thereby enriching the information available for analysis. This feature-centric approach provides an adaptable pipeline that can be readily integrated into various medical image processing systems without altering the core diagnostic workflow.

Future work will focus on evaluating the discriminative power of these extracted features across multiple datasets, optimizing feature selection strategies to reduce redundancy, and exploring automated feature learning techniques to complement the hand-crafted descriptors presented in this study.

REFERENCES

[1].GA Roth, GA Mensah, and V Fuster, "The global burden of cardiovascular diseases and risks: a compass for global action," *Journal of the American College of Cardiology*, 2020.

[2].F. Bray, M. Laversanne, E. Weiderpass, "The ever-increasing importance of cancer as a leading cause of premature death worldwide," Cancer, 2021.

[3].M. A. B. Khan, M. J. Hashim, H. Mustafa, M. Y. Baniyas, "Global epidemiology of ischemic heart disease: results from the global burden of disease study," Cureus, 2020.

[4].MD. Javeed and F. Jabeen, "FPGA Implementation for the Linking of Cell Tracks Using New Structure Algorithm," *International Journal of Engineering and Advanced Technology (IJEAT)*, vol. 9, no. 1, pp. 6773–6778, Oct. 2019.
https://www.ijeat.org/portfolio-item/a2976109119/

[5].M. Amini, F. Zayeri, and M. Salehi, "Trend analysis of cardiovascular disease mortality, incidence, and mortality-to-incidence ratio: results from global burden of disease study 2017," BMC public health, 2021.

[6].G. B. of C. D. Collaborators, "Global burden of cardiovascular diseases and risk factors, 1990–2019: update from the GBD 2019 study," Journal of the American, 2020.

[7].A. Giovanni, A. Enrico, B. Aime, "Global Burden of cardiovascular diseases and risk factors, 1990–2019: update from the GBD 2019 study," *Journal of the*, 2020.

[8].A. S. Kumar and N. Sinha, "Cardiovascular disease in India: A 360 degree overview," Medical Journal Armed Forces India, 2020.

[9].M. Senthil Kumar and M. Javeed, "Design of NoC Router with 3PE, Double and Triple Error Detection by Using Improved Hamming Code," *ARPN Journal of Engineering and Applied Sciences*, vol. 14, no. 16, pp. 2874–2880, Aug. 2019.
https://www.arpnjournals.org/jeas/research_papers/rp_2019/jeas_0819_7884.pdf
Google Scholar

[10]. M. Vaduganathan, G. A. Mensah, J. V. Turco, "The global burden of cardiovascular diseases and risk: a compass for future health," Journal of the America, 2022.

[11]. A. Author1, B. Author2, and C. Author3, "Global effect of modifiable risk factors on cardiovascular disease and mortality," Global Cardiovascular Risk … - New England Journal, 2023.

[12]. MD. Javeed and F. Jabeen, "FPGA Implementation for the Linking of Cell Tracks Using New Structure Algorithm," *International Journal of Engineering and Advanced Technology (IJEAT)*, vol. 9, no. 1, pp. 6773–6778, Oct. 2019.
https://www.ijeat.org/portfolio-item/a2976109119/

[13]. N. Townsend, D. Kazakiewicz, F. L. Wright, "Epidemiology of cardiovascular disease in Europe," Nature Reviews, 2022.

[14]. M. Heron, "Deaths: leading causes for 2019," 2021.

[15]. F. B. Ahmad and R. N. Anderson, "The leading causes of death in the US for 2020," Jama, 2021.

[16]. MD. Javeed and C. F. Jabeen, "Linking of Cell Tracks Using Segmentation," *International Journal of Innovative Technology and Exploring Engineering (IJITEE)*, vol. 9, no. 1, pp. 3020–3026, Nov. 2019.
https://www.ijitee.org/portfolio-item/A9128119119/
Google Scholar

[17]. MS Zimmerman, AGC Smith, CA Sable, et al., "Global, regional, and national burden of congenital heart disease, 1990–2017: a systematic analysis for the Global Burden of Disease Study 2017," The Lancet Child & Adolescent Health, 2020.

[18]. M Senthil Kumar and Md Javeed. An efficient rice variety identification scheme using shape, harlick & color feature extraction and multiclass svm. Int J Eng Adv Technol, 8(6):3629–3632, 2019.
https://www.ijeat.org/portfolio-item/f9362088619/
Google Scholar

[19]. M. F. Yuyun, K. Sliwa, A. P. Kengne, and A. O. Mocumbi, "Cardiovascular diseases in sub-Saharan Africa compared to high-income countries: an epidemiological perspective," Global, 2020.

[20]. Z. Su, Z. Zou, S. I. Hay, Y. Liu, S. Li, H. Chen, "Global, regional, and national time trends in mortality for congenital heart disease, 1990–2019: An age-period-cohort analysis for the Global Burden of Disease 2019," The Lancet, 2022.

[21]. S. Coffey, R. Roberts-Thomson, A. Brown, "Global epidemiology of valvular heart disease," *Nature Reviews*, 2021.

[22]. N. L. Bragazzi, W. Zhong, J. Shu, "Burden of heart failure and underlying causes in 195 countries and territories from 1990 to 2017," European Journal, 2021.
[23]. H. Dai, A. A. Much, E. Maor, E. Asher, "Global, regional, and national burden of ischaemic heart disease and its attributable risk factors, 1990–2017: results from the Global Burden of Disease Study 2017," European Heart, 2022.
[24]. M. Javeed and M. Senthil Kumar, “Automatic Brain Tumour Detection Using New Structure Algorithm,” *International Journal of Innovative Technology and Exploring Engineering (IJITEE)*, vol. 8, no. 11, pp. 3402–3405, Sep. 2019.
https://www.ijitee.org/portfolio-item/K25360981119/
Google Scholar
[25]. W. Wang, M. Hu, H. Liu, X. Zhang, H. Li, F. Zhou, and Y. M. Liu, "Global Burden of Disease Study 2019 suggests that metabolic risk factors are the leading drivers of the burden of ischemic heart disease," *Cell Metabolism*, 2021.
[26]. American Heart Association Council on Epidemiology, "Heart disease and stroke statistics—2023 update: a report from the American Heart Association," Circulation, 2023.
[27]. R. M. Haralick, K. Shanmugam and I. Dinstein, "Textural Features for Image Classification," in IEEE Transactions on Systems, Man, and Cybernetics, vol. SMC-3, no. 6, pp. 610-621, Nov. 1973, doi: 10.1109/TSMC.1973.4309314.
[28]. P. J. Costianes and J. B. Plock, "Gray-level co-occurrence matrices as features in edge enhanced images," 2010 IEEE 39th Applied Imagery Pattern Recognition Workshop (AIPR), 2010, pp. 1-6, doi: 10.1109/AIPR.2010.5759705.
[29]. Z. Abbas, M. Rehman, S. Najam and S. M. Danish Rizvi, "An Efficient Gray-Level Co-Occurrence Matrix (GLCM) based Approach Towards Classification of Skin Lesion," 2019 Amity International Conference on Artificial Intelligence (AICAI), 2019, pp. 317-320, doi: 10.1109/AICAI.2019.8701374.
[30]. M. Vidya and M. V. Karki, "Skin Cancer Detection using Machine Learning Techniques," 2020 IEEE International Conference on Electronics, Computing and Communication Technologies (CONECCT), 2020, pp. 1-5, doi: 10.1109/CONECCT50063.2020.9198489.